Indian Journal of Geography & Environment 13 (2014) 01-09

VIDYASAGAR UNIVERSITY

INDIAN JOURNAL OF GEOGRAPHY AND ENVIRONMENT

ISSN:0972-7388

Available online : http://vidyasagar.ac.in/journal

Modelling of Photosynthesis Vegetation Cover Fraction on Upscaling Approaches by using Landsat-8, AWiFs and MODIS Data

Ramprasad Kundu* and Abhisek Chakrabary

Department of Remote Sensing
Vidyasagar University, Medinipur, W.B.

ARTIC LE INFO

Articla history:
Received 04 August 2014
Received in revised form
09 September 2014
Accepted 10 October
2014

Keywords:
Landsat-8, Green vegetation fraction (GVF), Normalized difference vegetation index (NDVI), Dimidiate pixel model, Spectral mixture analysis (SMA).

ABSTRACT

Green Vegetation Fraction (GVF) is one of the most important land surface products to partition the fraction of the surface into evapo-transpiration and evaporation controlled by vegetation and bare soil respectively. Besides, GVF is a sensitive bio-indicator for identifying vegetation anomaly, land degradation and enhanced areas of moisture loading due to evapo-transpiration and input parameter for soil loss equation. Satellite Remote Sensing provides a seemingly obvious data source for quantifying GVF over large areas by virtue of multispectral capability and temporal repitivity. Based on the concept of Gutman and Ignatov (1998) mosaic pixel model Bingfang et al. (2004) developed an improved Dimidiate Pixel Model to estimate vegetation fraction using NDVI values of soil and vegetation after careful selection of thresholds. The main objective of the present study in mixed forest areas of Paschim Midnapur is to generate GVF from Landsat-8 data using Dimidiate pixel model and comparing with ground observation as well as on the concept of upscalling approach compared with estimated GVF values from AWiFs data and coarse resolution MODIS data. Altogether 26grids of 1000 x 1000 m size having different degree of ground vegetation cover are selected and the representative value of GVF was determined using Landsat-8 OLI sensor data. Time composite MODIS NDVI product of 1km was also used for comparative evaluation of prediction accuracy at different spatial scale with respect to measured GVF data. There is good agreement between GVF predicted from Landsat-8 and AWiFS data (R^2 = 0.93, RMSE = 3.11 and R^2 = 0.88, RMSE = 4.35) and MODIS NDVI products of 250m (R^2 = 0.79, RMSE = 5.93), whereas the correlation between MODIS NDVI products of 1km and measured values were less significant. The results show that Landsat-8 and time composite MODIS NDVI can predict GVF with reasonably good accuracy for large area at a time especially in deciduous forest areas. Poor correlation between MODIS NDVI products of 1km and ground observation could be due to coarse ground footprint of MODIS NDVI products of 1km data and data handling or data processing error.

*Corresponding Author

E-mail address : ramrsgis@gmail.com (R. Kundu)

1. Introduction

The Green vegetation Fraction (GVF) is acting an important role in the earth ecological system, and it affects the energy balance between the earth and atmosphere, being the nature "link". The vegetation growth has obvious seasonal variation characteristic, and become the "display" in the global climatic change (*Jiang et al, 2006*). Therefore research on the correlation between the vegetation and the climatic change has become very important in the global change research. Green vegetation fraction (GVF) defines an important structural property of a plant canopy, which corresponds to the complement to unity of the gap fraction at nadir direction, accounting for the amount of vegetation distributed in a horizontal perspective (*Xiao-Bing et al, 2003*). GVF is one of the major inputs to land surface products for partitioning of latent heat, soil and sensible heat fluxes under different proportion of ground cover. It plays a major role in energy and moisture exchanges across the earth's surface and atmosphere. Green vegetation fraction is considered as comprehensive quantitative variable for characterizing ecosystem and serves as a sensitive bio-indicator for identifying vegetation anomaly, areas of moisture loading, irrigation requirement and soil erodibility. Field measurement, as a traditional method of vegetation fraction, can be divided into three kinds of methods according to principles: field sample method, instrument method and visual estimation method (*Sutherland, 1999*). Traditional field measurement method to get the regional-scale vegetation fraction is very difficult due to the costs, labour and time involved. Furthermore, the reliability of some field measurement methods for the vegetation fractional coverage is questionable (*Curran et al, 1986*). Thus, traditional method is not feasible in regional-scale estimation of vegetation fraction. In order to calculate regional-scale estimation of vegetation fraction, we can utilize remote sensing technique. Space borne remote sensing technology provides a seemingly obvious choice for quantifying GVF over large areas. Satellite data provides a spatially and periodic, comprehensive view of land vegetation cover (*Chen Yunhao et al, 2001*). Data from remote sensing platforms are widely used for the analysis of vegetation conditions and provide significant information of vegetation fraction at regional scales. However, accuracy is limited because of their coarse ground footprint (*Roberts et al, 1993; Numata et al., 2008)*.

Although the digital camera can provide the GVF information in the plant quadrate with higher accuracy for a smaller range, it is unlikely to do so for a larger range. Remotely sensed data provides the possibility with three kinds of methods to measure the vegetation fractional coverage which are i) empirical regression formulation and vegetation index conversion method and ii) sub-pixel decomposition (*Zhou and Robson, 2001; Graetz, 1988; Dymond et al., 1992; Shoshany et al., 1996; Gutman and Ignatov, 1998*) and iii) linear spectral mixture models (*Wu and Peng, 2010*). The common remote sensing method is to use empirical regression formulation or vegetation index conversion method to estimate vegetation fraction. The empirical models comprised of normalized difference vegetation indices are mostly used due to their simplicity (*Ustin et al., 2004; Jiang et al., 2006*). Greetz et al., (1988) used the Landsat MSS band 5 data and field data to establish empirical relationship, and estimated the vegetation fraction in semi-arid region. Wittich and Hansing (1995) established the empirical model between the fractional vegetation cover (FVC) and NDVI for different land cover types, and calculated the FVC using the NOAA's Advanced Very High Resolution Radiometer (AVHRR) data. Purevdor et al. (1998) built four non-linear models by applying the empirical model, to assess the FVC in Mongolia and Japan's grassland areas. In addition, by establishing a quadratic polynomial relation between the FVC and vegetation index, grassland FVC can be more accurately estimated using AVHRR data. Quamby et al. (1992) established a mixed linear conversion model between vegetation index and the FVC, suitable for estimating the FVC in the agricultural area. Non-linear empirical relationship was developed between surface vegetation fraction and NDVI by Dymond et al. (1992). North (2002) also reported that multi-band linear mixing model from ATSR-2 data can predict fractional vegetation cover better than vegetation index. Based on the concept of Gutman and Ignatov (1998) mosaic pixel model Bingfang et al. (2004) developed an improved Dimidiate Pixel Model to estimate vegetation fraction using NDVI values of soil and vegetation after careful selection of thresholds. The method is suitable for getting the estimation of vegetation fraction in large scale region. The empirical model relies on in situ measurement data in specific regions, and the measured result is fairly accurate only if the study area is small. The accuracy will be substantially reduced in large scale application and monitoring as there will be many constraints. Compared to the regression model, the vegetation index is of a greater practical significance, as it does not need ground quadrate measuring over large areas,

and once verified, the model can be applied to large areas to formulate universally applicable calculation method for the GVF.

In the present study green vegetation fraction was measured for selected areas or mixed deciduous forest of Paschim Midnapur using high resolution data and compared with GVF derived from Landsat-8, AWiFS and MODIS to predict the impact of spatial resolution of sensors on upscaling of GVF.

2. Materials and Method

2.1 Study Area

The study was conducted over an area of Paschim Medinipur district, West Bengal, the geographic extent of which varies between 21°43'34"N to 22°57'15"N latitude and 86°30'57"E to 87°51'43"E longitude and covering the total area of 9295.28 sq. km. Out of this the total forest area is 1730.38 sq. km which constitutes about 18.62 percent of its total geographical area and net area under cultivation is 5852.22 sq. km. The district is situated in the south-western side of West Bengal, bounded by Bankura district and Purulia district in the north, Mayurbhanj district and Balasore district of Orissa in the south, Hooghly district and Purba Medinipur district in the east and Singhbhum district of Jharkhand and Purulia district of West Bengal in the west. The climate is tropical and the land surface of the district is characterised by hard rock uplands, lateritic covered

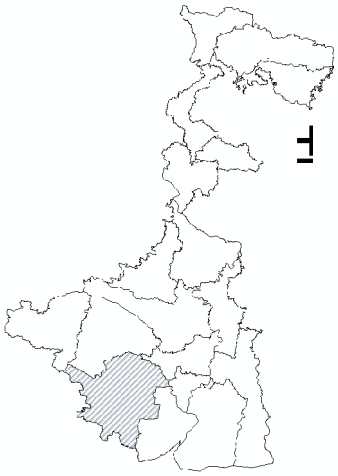

Fig. 1 : Location of study area

area, and flat alluvial and deltaic plains. Extremely rugged topography is seen in the western part of the district and rolling topography is experienced consisting of lateritic covered area. These rolling plains gradually merge into flat alluvial and deltaic plains to the east and south east of the district. The soil is fairly fertile. Normal rainfall is 1560 mm and average rainfall in the district is 1656 mm. The climate is characterized by hot summer, cold winter, abundant rainfall and humidity from 1450 mm to 1560 mm per year. Kangsabati, Silabati, Subarnarekha, Dulongs, Keleghai and their tributaries are the main rivers of the district. For agriculture Kangsabati canal system is the main irrigation scheme which is provided to both kharif and rabi crops.

2.2 Data Used

In the present study, different multi-sensor satellite data has been used to modelling of photosynthetic vegetation cover fraction. First of all, Landsat-8 data of path/row 139/44 and 139/45 of 20th November, 2013 with 16 days repitivity has been used which provide 30m spatial resolution. Resourcesat-2 AWiFS data of 56m spatial resolution of 20th November, 2011 (path/row: 107/56) was also used for calculation of GVF. Besides Terra MODIS NDVI product of 2nd fortnight of November with spatial resolution of 250m, 500m and 1km was used for comparative study, assuming that the vegetation fraction did not change significantly within study period.

2.3 Methodology

2.3.1 Landsat-8 Data Pre-processing

Landsat-8 OLI band data are converted to TOA planetary reflectance by using reflectance rescaling coefficients provided in the product metadata file (MTL file). The following equation is used to convert DN values to TOA reflectance for OLI data as follows:

$$\rho\lambda' = M_\rho Q_{cal} + A_\rho \quad \text{..... (1)}$$

Where:

$\rho\lambda'$ = TOA planetary reflectance, without correction for solar angle. Note that $\rho\lambda'$ does not contain a correction for the sun angle.

M_ρ = Band-specific multiplicative rescaling factor from the metadata

A_ρ = Band-specific additive rescaling factor from the metadata

Qcal = Quantized and calibrated standard product pixel values (DN)

TOA reflectance with a correction for the sun angle was then calculated by using the following equation:

$$\rho\lambda = \frac{\rho\lambda'}{\cos(\theta_{SZ})} = \frac{\rho\lambda'}{\sin(\theta_{SE})} \quad \text{..... (2)}$$

$\rho\lambda$ = TOA planetary reflectance

θ_{SE} = Local sun elevation angle. The scene center sun elevation angle in degrees is provided in the metadata (SUN_ELEVATION).

θ_{SZ} = Local solar zenith angle; $\theta_{SZ} = 90° - \theta_{SE}$

Table 1: Details of Data used for the Study

Data Product	Spatial Resolution	Temporal Resolution	Radiometric Resolution	Swath	Path/Row	Date of Acquisition
Landsat-8	30m	16 days	12 bit	185 km	139/44, 139/45	20th Nov, 2013
AWiFs	56m	5 days	10 bit	740 km	107/56	20th Nov, 2013
MODIS MOD13Q1	250m	16 Days	16 bit	2330 km	25/06, 26/06	2nd fortnight of Nov, 2013.
MODIS MOD13A1	500m	16 Days	16 bit	2330 km	25/06, 26/06	2nd fortnight of Nov, 2013.
MODIS MOD13A2	1000m	16 Days	16 bit	2330 km	25/06, 26/06	2nd fortnight of Nov, 2013.

2.3.2 AWiFs Data Pre-processing

2.3.1.1 Radiometric Calibration

The DN value converted to radiance value by using the following formula:

$$L^{*} = \frac{(L_{\max} - L_{\min})}{Q_{cal\max}} Q_{cal} + L_{\min} \quad \text{..... (3)}$$

Where,

L^{*} = spectral radiance at the sensors aperture W/ (m^2.sr.um)

Q_{cal} = Calibrated Digital Number

Q_{calmax} = maximum possible DN value

L_{max} & L_{min} = scaled spectral radiance

2.3.1.2 Geometric Correction

AWiFs dataset was registered geometrically using Survey of India (SOI) topomaps of 1:50,000 scale. About 60 well distributed Ground Control Points (GCPs) were identified as tie points, keeping in view root mean square error of less than one pixel. The image was geo-referenced using 2nd polynomial function and nearest neighbourhood resampling technique. The AWiFS data was projected to geographic lat-long with WGS84 datum.

2.3.2 Vegetation Indices based on NDVI

The Normalized Difference Vegetation Indices (NDVI) is mainly based upon the different behaviours exhibited by the vegetation toward different electromagnetic wavelengths: the chlorophyll inside the vegetation absorbs the energy situated within the red wavelength, while the mesophyll reflects back the infrared segment. Both the chlorophyll and mesophyll are essential elements in the photosynthesis process for plants. NDVI is one of the most commonly used vegetation indices due to its simplicity in calculation and minimum impact of surface topography and illumination geometry. It is the linear combination of red and infrared band and a surrogate indicator of plant vigour. It is highly correlated with vegetation parameters such as green leaf biomass and green leaf area and hence is of considerable value for vegetation segmentation (*Curran & Franquin, 1980; Holben & Frasher, 1984; Jackson et al., 1983; Justice et al., 1985*) which is highly valuable in continental studies. An NDVI vegetation index from Landsat-8 and AWiFs data was calculated as follows:

$$NDVI = (R_{IR} - R_R) / (R_{IR} + R_R) \quad \text{..... (4)}$$

Where, R_{IR} = spectral reflectance in the infrared region and R_R = spectral reflectance in the red region. The value of NDVI varies between -1 and +1. Band 5 and band 4 of Landsat-8 and Band 3 and band 2 of AWiFS data were used for calculation of NDVI.

2.3.3 Dimidiate Pixel Model (DPM)

Dimidiate pixel model (DPM) is based on spectral mixture analysis (SMA) that assumes linear decomposition of the spectral signal received from a ground pixel is the sum of the fractional abundance of pure soil and pure vegetation in the mixed pixel and the contribution by vegetation in the mixed pixel is expressed as:

$$S = f_c \times S_{veg} + (1 - f_c) S_{soil} \quad \text{..... (5)}$$

Where,

S = signal received by the remote sensor

fc= the vegetation fraction

1- fc= the soil fraction

S_{veg}= the signal of a pure vegetation pixel

S_{soil}= the signal of a pure soil pixel

2.3.4 Establishment of Remote Sensing Model

The DPM is a practical approach for modelling of photosynthetic vegetation cover fraction as it is simple to compute and assumes that the surface of a pixel is covered with vegetation and non-vegetation. The NDVI is also a type of quantitative value calculated from spectral information of surface objects received from remote sensors and reflects the condition of surface

vegetation. Hence equation 5 can be re-written in terms of NDVI as:

$$f_c = \frac{(NDVI - NDVI_{soil})}{(NDVI_{veg} - NDVI_{soil})} \quad \text{..... (6)}$$

Where, S_{soil} and S_{veg} are the spectral responses from pure soil and pure vegetation pixels, respectively. Major advantage of the dimidiate pixel model is that the impacts from atmosphere, soil background and vegetation type are reduced (*Zhang et al., 2012*).

The $NDVI_{soil}$ value of most bare soil surfaces is close to zero in theoretical basis. Most of cases due to the impact of many factors $NDVI_{soil}$ values range between 0.1 and 0.2. $NDVI_{veg}$ represents the maximum value of the pure vegetation pixel. However, $NDVI_{veg}$ also changes with time and space due to the effect of different vegetation types *(Xiao-Bing et al., 2003)*. Therefore, the determination of $NDVI_{soil}$ and $NDVI_{veg}$ values has become a critical issue in this model. Here in the study, the values of $NDVI_{soil}$ and $NDVI_{veg}$ were averaged to produce two unique values. There were marginal difference in $NDVI_{soil}$ as the soil moisture regime and surface condition was almost uniform across the study area. In the present study from Landsat-8 the values of NDVIveg and NDVIsoil are computed to be 0.542 and 0.171 and on the other hand from AWiFs data the values of $NDVI_{veg}$ and $NDVI_{soil}$ are computed to be 0.502 and 0.151 respectively.

2.3.5 Vegetation Cover Measurements in the Ground

Field measurement of pixel points is the conventional method to estimate the accuracy of vegetation cover fraction. But in this study it was hardly to survey the vegetation cover fraction in a unit as large as 56 m multiplied by 56 m, or 250 m multiplied by 250 m. So a new solution for vegetation covers measurements in the field altogether 60 grids of 1000m x 1000m size having different degree of ground vegetation cover are selected by using the grid box which represents the 1000m each in ground area in deciduous forest of Paschim Medinipur district, where Sal (*i.e. Shorea robusta*) is the main type of vegetation. For measurement of ground cover by vegetation, vertical photograph of fields were taken from Google Earth as an image tile keeping the height of approximately 1.63km which was adopted for sampling. The 60 image tiles were imported into ERDAS imagine (ver. 9.0) for processing and registered by using the rectified vector grid box. Unsupervised classification was performed and each registered image tiles were classified into 25 classes. Further the 25 classes were generalized into green vegetation and non-vegetation classes through visual interpretation to compute vegetation fraction. The green vegetation fraction was calculated as number of green pixels divided by total pixels within the respected image tile and expressed as percentage which is the representative value of GVF. A total number of 26 image tile samples were selected out of digitally classified 60 image tile samples, which were used for GVF model validation.

2.3.6 Comparative Studies by using MODIS 250m, 500m, 1km Data

On the concept of upscalling approach MODIS L-2 NDVI products of 250m, 500m and 1km resolution of 16-day composite was downloaded from in HDF format and care was taken such that there is minimum time gap across all the datasets under study. These NDVI data were already adjusted through the radiation method, geography localization and atmospheric adjustment. NDVI data was re-projected from a sinusoidal to Geographic lat-long projection with WGS84 datum, using a nearest neighbour resampling routine. Then the above described methodology was applied to the NDVI data of MODIS to predict the GVF and setup a correlation study with field observation.

3. Result and Discussion

3.1 Measurement of Ground Vegetation Cover from High Resolution Satellite data

Summary statistics of measured green vegetation fraction of 26 reference grids is given in Table 2. The proportion of vegetation cover varies from 24.90% to as high as 74.72% with mean value of 62.12% (± 12.08) across all the grids as the area was sampled based on high, medium and low surface cover. It is also noted that the ground cover of the reference grids is mostly greater than 50% except two.

3.2 GVF Estimation based on Landsat-8 Data

NDVI was calculated from the Landsat-8 data by using the Landsat NDVI equation. $NDVI_{veg}$ and $NDVI_{soil}$ were computed from Landsat-8 data by using zonal statistics and calculated $NDVI_{soil}$ value was 0.171 which present a big significance on vegetation fraction estimation. The lowest NDVI value of 0.171 represents 26.77% GVF and as high value of GVF 75.67% estimated at highest NDVI value. The distribution of GVF predicted from landsat-8 is given in Fig. 2a. The calculated GVF from Landsat-8 was compared with measured GVF. The scatter plot (fig. 3a) shows a well degree of agreement ($R^2 = 0.933$) with higher degree of sensitivity and it is also highly correlated with vegetation fraction. The correlation also presents the

relationship with other parameters such as green leaf biomass, green leaf area and it is of considerable value for vegetation segmentation or vegetation fraction.

3.3 GVF Estimation based on AWiFS Data

NDVI was calculated from the AWiFS data using equation 4. The scene specific values of $NDVI_{veg}$ and $NDVI_{soil}$ were computed to be 0.502 and 0.151 respectively. The range of NDVI values vary from 0.151 at 30.99% GVF to as high as 0.502 at 73.708% GVF with average value of 0.33 (±0.25). Spatial depiction of GVF is given in Fig. 2b. GVF calculated from AWiFS was compared with measured GVF. The scatter plot between measured and predicted GVF (Fig. 3b) shows fairly well degree of agreement (R^2 = 0.882) with higher degree of sensitivity. The scatter plot shows slight underestimation of below 50% GVF which could be due to pixel size and boundary pixels which cut across the reference grid.

3.4 GVF Estimation based on Course Resolution 250m MODIS Data

MODIS GVF was generated using 16 days composite 250m NDVI product. Similar to AWiFS data scene specific values of $NDVI_{veg}$ and $NDVI_{soil}$ were determined to be 0.81 and 0.24 respectively. The range of GVF values vary from 35.21% to 71.75% based on DPM. Spatial distribution of GVF values derived from MODIS data is given in Fig. 2c. The scatter plot between measured and predicted GVF (Fig. 3c) shows significant positive correlation (R^2 = 0.787) albeit lower than AWiFS. The scatter plot shows slight underestimation of GVF below 40% which could be due to pixel size and time composite NDVI product.

3.5 GVF Estimation based on Course Resolution 500m MODIS Data

Based on the concept of data upscaling approaches MODIS GVF was generated using 500m NDVI product which was 16 days NDVI composite based on MVC technique. Same as the above scene specific values of NDVIveg and NDVIsoil were calculated to be 0.87 and 0.25 respectively. Based on dimidiate pixel model GVF has been estimated from the range of 41.79% GVF as low to 72.02% GVF as high value. Spatial distribution of GVF values derived from MODIS data is given in Fig. 2d. The scatter plot between measured and predicted GVF (Fig. 3d) shows correlation significance (R^2 = 0.714) which is strongly positive in respect of measured GVF.

3.6 GVF Estimation based on Course Resolution 1km MODIS Data

To compare the relation with data upscaling approaches MVC composite 16days NDVI product of 1km has been used to predict the GVF values. Upscaling the data from small scale to large scale, GVF has been calculated in respect of the range of NDVI values which vary from 34.0% GVF to as high as 78.17% GVF. The correlation between measured and predicted GVF values represents the positive correlation (R^2 = 0.628) though the correlation significance is not so better which may be due to large ground footprint and could be due to pixel size and time composite NDVI product but for large scale

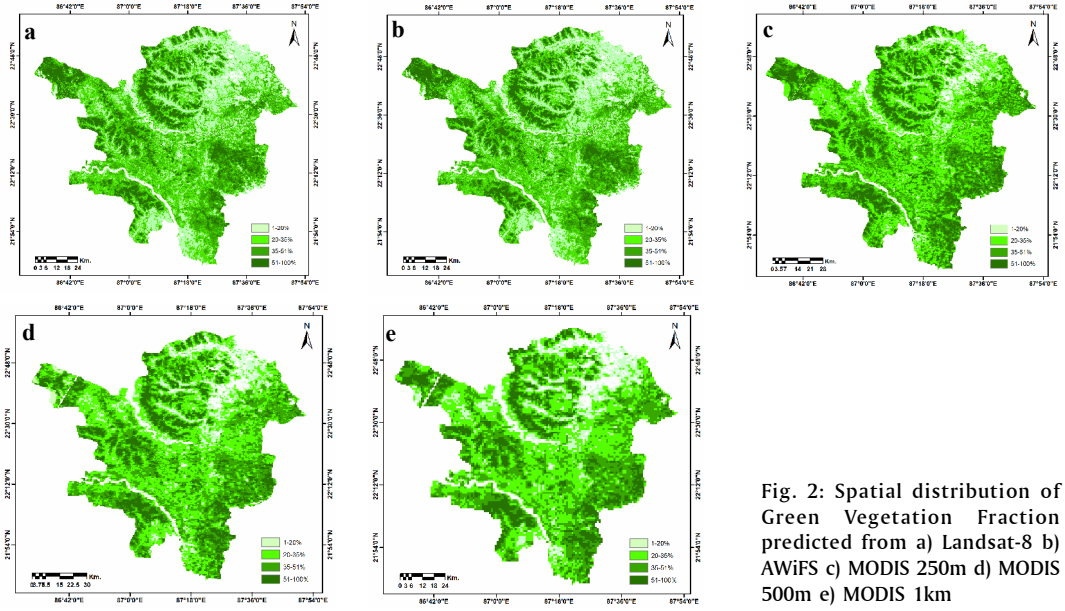

Fig. 2: Spatial distribution of Green Vegetation Fraction predicted from a) Landsat-8 b) AWiFS c) MODIS 250m d) MODIS 500m e) MODIS 1km

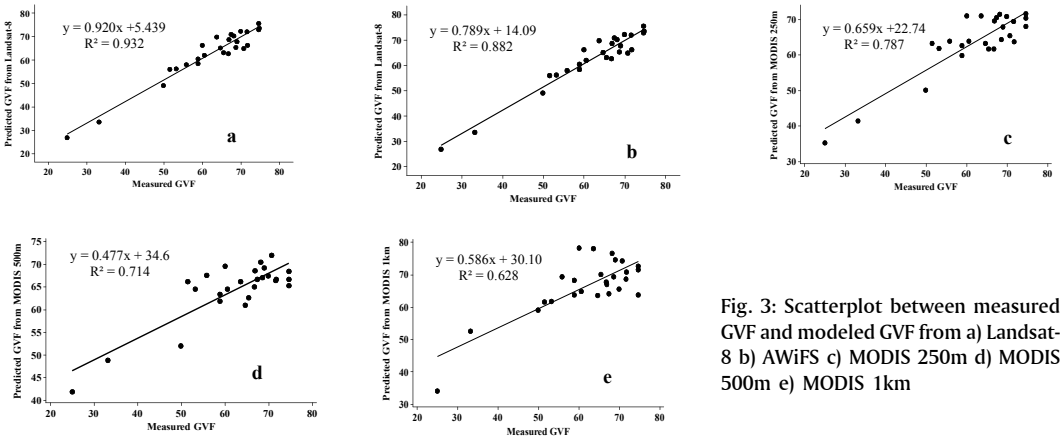

Fig. 3: Scatterplot between measured GVF and modeled GVF from a) Landsat-8 b) AWiFS c) MODIS 250m d) MODIS 500m e) MODIS 1km

Table 2: Summary statistics of GVF values

GVF	Min	Max	Mean	SD	R^2	RMSE
Measured	24.90	74.72	62.12	12.08	-	-
Landsat-8	26.77	75.67	62.62	3.11	0.97	0.932
AWiFS	30.99	73.71	63.15	4.35	0.94	0.881
MODIS 250m	35.21	71.75	63.69	5.93	0.89	0.787
MODIS 500m	41.79	72.02	64.26	7.46	0.84	0.713
MODIS 1km	34.00	78.17	66.55	8.49	0.79	0.627

study this is so much important. The scatter plot represents their relationship between measured and estimated GVF from MODIS NDVI product of 1km in Fig 3e and spatial distribution of GVF is represents in Fig 2e.

3.7 Comparison of Measured GVF with Modelled GVF

The above discussed methodology and result is based on the concept of data upscalling approaches where was upscalled from large scale to small scale on regional basis. There could be several types of error but based on this concept data analysis on regional scale is possible. In our present study, comparison of measured GVF with modelled GVF derived from coarse resolution satellite data reveals that RMSE error is minimum (3.11) in Landsat-8 derived GVF data whereas the error is significantly high in both MODIS 500m NDVI product (7.46) and MODIS 1km NDVI product (8.49). There could be several reasons for high values of RMSE and poor coefficient of determination. The inherent shortcomings could be comparison between single date data and time composite product, secondly the accuracy with which the soil and vegetation NDVI values have been used for calculation of GVF and thirdly the coarser ground footprint. But the purpose of the present study was aimed at upscaling at regional scale and the GVF prediction ability across sensors. One of the assumption of this study is that the forest canopy cover does not change significantly within a fortnight but it may not be so especially in mixed deciduous forest of Paschim Midnapur. It was apparent from the present study that with decrease in spatial resolution the predictability decrease, however, for medium resolution data like Landsat-8 and AWiFS the prediction is within acceptable limit.

4. Conclusion

Green vegetation fraction is an important component in energy partitioning in terms of sensible and latent heat flux over terrestrial ecosystem. The GVF product also aid in identifying vegetation anomaly, areas of moisture loading due to evapo-transpiration and serve as an input parameter to soil loss equation. Due to the limitations of field based estimation, satellite

remote sensing at higher temporal and spatial scale is only seemingly possible approach to estimate GVF for operational use. In the present study deciduous forest ecosystem was chosen to measure the green vegetation cover using very high resolution satellite data as a surrogate of field measurement and was upscaled at different spatial scale to evaluate the predictability by different sensors ranging from 30m to 1000m. GVF of single date Landsat-8 data, AWiFs data and time composite MODIS NDVI products were compared with measured values for predictive ability. GVF derived from single date Landsat-8 data gave higher correlation in comparison to AWiFs and MODIS data and also the root mean square error was minimum. Less significant correlation was observed between measured Landsat-8 and MODIS 1km GVF and the RMSE was also slightly high. The slope between measured and predicted GVF, representing sensitivity, decreases with decrease in spatial resolution. The factors causing large variability could be thresholding of input parameters in Dimidiate Pixel Model and single date verses time composite product. Although it was presumed that the canopy architecture and ground cover will not change significantly over a short period of time but it may not be so under mixed deciduous forest condition. As the study was carried over a limited period and area, further analysis is required considering time synchronized data acquired over different ecosystems along with actual ground measurement.

Acknowledgements

Authors are thankful to Dr D. Dutta, General Manager of RRSC-East/ISRO for providing the kind guidance and technical facility to carry out the study. We would also like to acknowledge Dr. V K Dadhwal, Director of ISRO for constant support and useful suggestions during the course of research. Thanks are also due to Ms Prachi and Ms Manisha for their assistance at various stages of the study.

References

Bingfang Wu, Miaomiao Li, Changzhen Yan and Weifeng Z (2004). Developing method of vegetation fraction estimation by remote sensing for soil loss equation. Geoscience and Remote Sensing Symposium 2004, IGARSS '04, Proceedings, 2004 IEEE International, vol 6, pp 4352-4355.

Chen YH, Li XB and Shi PJ (2001). The study of vegetation cover dymatic monitoring by remote sensing of HaiDian District Beijing. *Botanic ecological transaction* 25(5): 588–593.

Curran PJ and Franquin P (1980). Multispectral remote sensing of vegetation amount. *Progress in Physics of Geography* 4: 315-341.

Curran PJ and Williamson HD (1986). Sample size for ground and remotely sensed data. *Remote Sens Environ* 20: 31-41.

Dymond JR, Stephens PR, Newsome PF and Wilde RH (1992). Percent vegetation cover of a degrading rangeland from SPOT. *Int J Remote Sens* 13: 1999-2007.

Graetz RD, Pech RR and Davis AW (1988). The assessment and monitoring of sparsely vegetated rangelands using calibrated Landsat data. *International Journal of Remote Sensing* 9(7): 1201–1222.

Gutman G and Ignatov A (1998). The derivation of the green vegetation fraction from NOAA/AVHRR data for use in numerical weather prediction models. *International Journal of Remote Sensing* 19: 1533-1543.

Holben BN and Fraser RS (1984). Red and near infrared response to off nadir viewing. *International Journal of Remote Sensing* 5: 145-160.

Holben BN (1986). Characteristic of maximum value composite images for temporal AVHRR data. *International Journal of Remote Sensing* 7(11): 1417–1434.

Jackson RD, Slater PN and Pinter PJ (1983). Discrimination of growth and water stress in wheat by various vegetation indices through clear and turbid atmospheres. *Remote Sensing of Environment* 15: 187-208.

Jiang Z, Huete AR, Chen J, Chen Y, Li J, Yan G and Zhang X (2006). Analysis of NDVI and scaled difference vegetation index retrievals of vegetation fraction. *Remote Sensing of Environment* 101: 366–378.

Justice CO, Townshend JRD, Holben BN and Tucker CJ (1985). Analysis of the phenology of global vegetation using meteorological satellite data. *International Journal of Remote Sensing* 6: 1271-1381.

North PRJ (2002). Estimation of fAPAR, LAI, and vegetation fractional cover from ATSR-2 imagery. *Remote Sensing of Environment* 80(l): 114–121.

Numata I, Roberts DA, Chadwick OA, Schimel JP, Galvao LS and Soares JV (2008). Evaluation of hyperspectral data for pasture estimation in the Brazillian Amazon using field and imaging spectrometers. *Remote Sensing of Environment* 112: 1569-1583.

Purevdor JTS, Tateishi R and Ishiyama T (1998). Relationships between percent vegetation cover and vegetation indices. *International Journal of Remote Sensing* 19(18): 3519–3535.

Quamby NA, Townshend JRG and Settle JJ (1992). Linear mixture modelling applied to AHVRR data for crop area estimation. *International Journal of Remote Sensing* 13(3): 415–425.

Roberts DA, Smith MO and Adams JB (1993). Green vegetation, nonphotosynthetic vegetation, and soils in AVIRIS data. *Remote Sensing of Environment* 44(2–3): 255-269.

Rouse JW, Haas RH, Schell JA and Deering DW (1973). Monitoring vegetation systems in the Great Plains

with ERTS. Proceedings of the 3rd ERTS Symposium NASA SP-351, Vol. 1, pp 48–62.

Shoshany M, Kutiel P and Lavee H (1996). Monitoring temporal vegetation cover changes in Mediterranean and arid ecosystems using a remote sensing technique: case study of the Judean Mountain and the Judean Desert. *Journal of Arid Environments* 33: 9–21.

Sobrino JA, Jiménez-Muñoz JC, Sòria G, Romaguera M, Guanter L, Moreno J, Plaza A, Martínez P (2008). Land Surface Emissivity Retrieval from Different VNIR and TIR Sensors. *IEEE Transactions on Geoscience and Remote Sensing* 46(2): 316-327.

Sutherland WJ and Zhang JT (1997). Manual of Survey Methods in Ecology. *Beijing: Science and Technology Literature Press.*(in Chinese j

Ustin SL, Roberts DA, Gamon JA, Asner GP and Green RO (2004). Using imaging spectroscopy to study ecosystem processes and properties. *Bioscience* 54: 523-534.

Wittich KP and Hansing O (1995). Area-averaged vegetative cover fraction estimated form satellite data. *International Journal of Biometeorology* 38(3): 209–215.

Wu J and Peng D (2010) A research on extracting information of the arid regions' vegetation coverage using improved model of spectral mixture analysis. Multimedia Technology, (ICMT), 1–5.

Xiao-Bing L, Yun-Hao C, Pei-Jun S and Jin C (2003). Detecting Vegetation Fractional Coverage of Typical Steppe in Northern China Based on Multi-scale Remotely Sensed Data. *Acta Botanica Sinica* 45(10): 1146- 1156.

Zhang X, Liaoa C, Li J and Sun Q (2013). Fractional vegetation cover estimation in arid and semi-arid environments using HJ-1 satellite hyperspectral data. *Int. J. Appl. Earth Observ. Geoinf* 21: 206-512.

Zhou Q, Robson M and Pilesjo P (1998). On the ground estimation of vegetation cover in Australian rangelands. *Int J Remote Sens* 9: 1815-1820.